Carbohydrate Polymers 85 (2011) 65–74

Contents lists available at ScienceDirect

Carbohydrate Polymers

journal homepage: www.elsevier.com/locate/carbpol

Starch transformation in bran-enriched extruded wheat flour

Frédéric Robin[a,c,*], Christine Théoduloz[a], Alessandro Gianfrancesco[a], Nicolas Pineau[b], Heike P. Schuchmann[c], Stefan Palzer[d]

[a] Department of Food Science & Technology, Nestlé Research Center, P.O. Box 44, 1000 Lausanne 26, Switzerland
[b] Department of BioAnalytical Science, Nestlé Research Center, P.O. Box 44, 1000 Lausanne 26, Switzerland
[c] Institute of Process Engineering in Life Sciences, Karlsruhe Institute of Technology (KIT), Kaiserstrasse 12, 76131 Karlsruhe, Germany
[d] Nestlé Product Technology Centre York, P.O. Box 204, Haxby Road, York YO91 1XY, United Kingdom

ARTICLE INFO

Article history:
Received 23 October 2010
Received in revised form 18 January 2011
Accepted 26 January 2011
Available online 26 February 2011

Keywords:
Cooking extrusion
Cereals
Starch
Dietary fibers
Material properties
Glass transition
Amorphous state

ABSTRACT

Wheat flour was extruded at different conditions of barrel temperature (120 °C and 180 °C), water content (18% and 22%) and screw speed (400 rpm and 800 rpm) with an increasing concentration of wheat bran fibers (2.8%, 12.6% and 24.4%). In the tested extrusion conditions, starch crystallites were fully dissociated. The estimated starch solubility was influenced by the process conditions and ranged from 24.1% to 63.1%. At same process conditions, the starch solubility was increased only at the highest bran level. The bran concentration influenced the glass transition temperature, melting temperature and sorption isotherm of the unprocessed wheat flour. At the extrusion conditions, it showed that higher bran levels led to a higher amount of free water and a decrease in starch glass transition temperature of up to 13 K. The differences in starch transformation, induced by the concentration of bran, might contribute to the modulation of the expansion properties of bran-containing starchy foams.

1. Introduction

Enrichment of extruded direct expanded starchy foods with dietary fibers is a major trend in the food industry in response to the consumer demand for healthier products. Wheat bran is a readily available and low cost by-product of the wheat grain refining process. It contains a high amount of dietary fibers, reported to bring nutritional and health benefits (Marlett, McBurney, & Slavin, 2002). However, incorporation of wheat bran in extruded products is still limited due to its negative effect on expansion (e.g. Yanniotis, Petraki, & Soumpasi, 2007; Brennan, Monro, & Brennan, 2008). The expansion mechanisms of cereal-based extruded products are mainly governed by the physicochemical properties of the plasticized starch matrix. These properties are modified during extrusion depending on the process conditions (e.g. Alvarez-Martinez, Kondury, & Harper, 1988). At same process parameters, addition of bran may modulate the physicochemical properties of the extruded starch and contribute to the observed changes in expansion properties. This may be caused by changes in the starch melting and glass transition temperatures due to competition for water, modification of the matrix melt viscosity and/or protection of starch granules against shear when increasing the bran concentration. To investigate these different hypotheses, starch transformation was assessed according to the bran concentration using complementary physicochemical tests: water solubility and absorption indices, gelatinization temperature of starch, starch pasting properties and molecular size distribution, glass transition and melting temperatures as well as the sorption isotherms. To investigate the effect of extrusion on fiber properties, the total, soluble and insoluble dietary fiber contents were measured.

2. Materials and methods

2.1. Material

Wheat flour type 550 and wheat bran, obtained by dry milling from the same source of grain, were provided by Provimi Kliba S.A. (Cossonay, Switzerland). Wheat bran (51.4% fibers) was added to the refined wheat flour (RF) (2.8% fibers) to achieve two lev-

Abbreviations: d.m., Dry matter; DSC, Dynamic Scanning Calorimeter; HB, High Bran; IDF, Insoluble Dietary Fibers; LB, Low Bran; LSD, Least Significant Difference; RF, Refined Flour; RVA, Rapid Visco Analyzer; SDF, Soluble Dietary Fibers; SME, Specific Mechanical Energy; SWS, Estimated Starch Water Solubility; TDF, Total Dietary Fibers.

* Corresponding author at: Department of Food Science & Technology, Nestlé Research Center, P.O. Box 44, 1000 Lausanne 26, Switzerland. Tel.: +41 21 785 9573; fax: +41 21 785 8554.
E-mail address: frederic.robin@rdls.nestle.com (F. Robin).

0144-8617/$ – see front matter © 2011 Elsevier Ltd. All rights reserved.
doi:10.1016/j.carbpol.2011.01.051

Nomenclature

a_w	water activity
C	constant
D	screw diameter
ΔH_u	enthalpy of fusion of the polymer per repeating unit
K	GAB constant
k	G&T constant
L	Barrel length
M	motor torque
m_{total}	total mass flow rate
M_{unload}	unload motor torque
n_{act}	actual screw speed
n_{max}	maximum screw speed
P_{max}	maximum motor power
T_d	die temperature
T_{pk}	melting temperature measured at the peak of the endothermic transition
$T_{g,onset}$	glass transition temperature measured at the onset of the transition
$T_{g,m}$	glass transition of fully dried material
$T_{g,w}$	glass transition of pure water
T^0_{pk}	melting temperature of the dry material
υ	volume fraction of water
V	molar volumes of water and polymer
η	RVA peak viscosity
W	water content
WAI	water absorption index
WSI	water solubility index
W_m	monolayer water content
χ_{12}	Flory–Huggins interaction polymer-diluant parameter

els of fiber content, 12.6% (thereafter LB for low bran) and 24.4% (thereafter HB for high bran) (AOAC 985.29). The increase in fiber resulted in an increase in proteins from 13.0 to 13.9 and 15.0% (AOAC 997.06), in fat from 1.1% to 1.6% and 2.2% (AOAC 983.23) and in ash from 0.8% to 1.8% and 3.2% (AOAC 923.03), respectively for the three recipes. The starch content decreased from 78.5% to 69.7% and 55.5% (obtained by difference from the other recipe components), respectively (all values are given in dry matter). Wheat bran was used at two levels of particle size, obtained by hammer milling: fine and coarse with an average diameter (volume weighted) of 224 μm ± 6 μm and 317 μm ± 1 μm (measured in Medium-chain triglyceride oil, Renens, Switzerland using a Mastersizer 2000, Malvern, Germany), respectively.

2.2. Extrusion experiments

A co-rotating double screw extruder (Evolum 25, Clextral, Firminy, France) with a barrel length of 400 mm (L) and a screw diameter of 25 mm (D) was used ($L/D = 16$). The screw configuration was composed of conveying and mixing elements with reverse elements in the last section of the barrel. Melt pressure and temperature (T_d) were measured after the fourth barrel zone and before the die with a pressure sensor (Kistler 4090B, Kistler Instrument A.G., Winterthur, Switzerland) and a type J thermocouple (ROTH+CO. A.G., Oberuzwil, Switzerland). The extruder was operated at a constant feed rate of 10 kg h^{-1}. The three first heating zones of the barrel were kept at a temperature of 40 °C, 80 °C and 120 °C, respectively. The screw speed, last barrel zone temperature and feed water content were modulated according to an experimental plan (Table 1). Wheat flour was mixed with wheat bran prior to extrusion in a powder mixer (Prodima MJ50, Mecatex/Prodima, St. Sulpice, Switzerland) and fed into the extruder using a co-rotating twin-screw feeder (K-Tron Co, Niederlenz, Switzerland). Water (20 °C ± 2 °C) was injected into the extruder at a controlled flow rate with a syringe pump (Teledyne ISCO 500D, Teledyne Isco Inc. Lincoln, Nebraska, USA).

The specific mechanical energy (SME) was calculated as follows:

$$\mathrm{SME} = \frac{(n_{act}/n_{max}) \times M - (n_{act}/n_{max}) \times M_{unload}}{m_{total}} \times P_{max} \quad (1)$$

where M and M_{unload} are the motor torque (in Nm) under load and without load, n_{act} and n_{max} are the actual and maximum screw speed, m_{total} is the mass flow rate and P_{max} is the maximum engine power (27 kW). A circular die of 10 mm length and 3.2 mm diameter was used. The samples were collected and dried at 60 °C for 16 h.

2.3. Starch characterization

2.3.1. Water solubility and absorption Indices

Water solubility index (WSI) and water absorption index (WAI) were determined using the method of Anderson, Conway, Pfeifer, and Griffin (1969). The extruded samples were ground and sieved through a 250 μm mesh. Samples (2.5 g) were dispersed in 30 mL of deionised water, agitated at room temperature (22 °C ± 1 °C) for 30 min and centrifuged at 9000 × g at 25 °C for 15 min. WAI and WSI measurements were duplicated and calculated as follows:

$$\mathrm{WAI} = \frac{\text{Wet pellet weight}}{\text{Sample dry weight}} \quad (2)$$

$$\mathrm{WSI} = \frac{\text{Supernatant dry solid weight}}{\text{Sample dry weight}} \times 100 \quad (3)$$

The percentage of starch solubility in water (SWS) (22 °C ± 1 °C) was estimated according to the following equation:

$$\mathrm{SWS} = \frac{\mathrm{WSI}}{\text{Percentage of total starch in dry sample}} \times 100 \quad (4)$$

2.3.2. RVA pasting profiles

Pasting profiles of extruded samples were evaluated using a Rapid Visco Analyzer (RVA-4, Newport Scientific, Jessup, MD). Ground extruded samples (<250 μm, 20% d.m. 0.1 M $AgNO_3$) were left 15 min at room temperature prior to measurement to allow hydration of the solid material. The samples were hold 1 min at 50 °C, heated to 95 °C at 11 K min^{-1}, held at 95 °C for 3 min and cooled to 50 °C at 6.5 K min^{-1} under stirring at 160 rpm. The peak viscosity (η) and corresponding time was recorded using the Thermocline software (v. 2.2, Newport Scientific, Jessup, MD). Measurements were duplicated.

2.3.3. Starch gelatinization temperature

Starch gelatinization temperature was measured in excess of water (ratio ground sample/water of 1:3, sealed mid-pressure aluminum pan (Mettler Toledo, Greifensee, Switzerland)) using a dynamical differential scanning calorimeter (DSC 823e, Mettler Toledo, Greifensee, Switzerland). The samples were heated from −5 °C to 160 °C at 5 K min^{-1}. The thermographs were analyzed with Star System® v.9.01 software (Mettler Toledo, Switzerland). The dissociation temperature of starch crystallites was determined at the transition peak.

2.3.4. Molecular size distribution of starch

Starch molecular size distribution was obtained by gel permeation chromatography. Approximately 200 mg of sample (starting material and ground extruded material) were hydrated in 1 mL of deionized water for 15 min. After adding 10 mL of dimethylsulfoxide the sample was heated in a boiling water bath for 15 min and

Table 1
Extrusion conditions and extruded material properties.

	Barrel temp. (°C)	Feed water content (% w.b.)	Screw speed (rpm)	Bran particle size	Fiber content (% d.b.)	SME (kJ kg^{-1})	WSI (% d.b.)	Estimated water soluble starch (SWS) (% d.b.)	RVA peak viscosity (cP)
RF1	120	18	400			506 ± 5	34.2 ± 0.3	43.6 ± 0.4	220 ± 20
RF2	120	18	800			607 ± 11	41.5 ± 0.1	52.9 ± 0.2	124 ± 4
RF3	120	22	400			371 ± 9	31.8 ± 0.5	40.5 ± 0.4	314 ± 28
RF4	120	22	800			449 ± 6	35.6 ± 0.2	45.3 ± 0.3	146 ± 4
RF5	180	18	400			319 ± 3	33.0 ± 0.3	42.0 ± 0.4	289 ± 16
RF6	180	18	800			454 ± 9	32.9 ± 0.0	42.0 ± 0.1	138 ± 6
RF7	180	22	400			233 ± 5	24.3 ± 0.1	30.9 ± 0.2	413 ± 11
RF8	180	22	800			280 ± 6	21.3 ± 0.7	27.1 ± 0.9	446 ± 1
LB1	120	18	400	Fine	12.6	559 ± 6	30.6 ± 0.4	44.1 ± 0.8	197 ± 11
LB2	120	18	800	Coarse	12.6	630 ± 18	36.9 ± 0.3	53.2 ± 0.7	158 ± 14
LB3	120	22	400	Coarse	12.6	430 ± 5	26.7 ± 0.3	38.5 ± 0.6	200 ± 3
LB4	120	22	800	Fine	12.6	511 ± 7	30.8 ± 0.2	44.4 ± 0.6	135 ± 6
LB5	180	18	400	Coarse	12.6	394 ± 4	29.3 ± 0.2	42.2 ± 0.5	166 ± 14
LB6	180	18	800	Fine	12.6	516 ± 9	35.0 ± 0.2	50.4 ± 0.5	105 ± 6
LB7	180	22	400	Fine	12.6	271 ± 3	22.3 ± 0.3	32.1 ± 0.6	261 ± 4
LB8	180	22	800	Coarse	12.6	406 ± 5	23.7 ± 0.0	34.2 ± 0.3	242 ± 7
HB1	120	18	400	Coarse	24.4	587 ± 6	21.8 ± 0.3	40.2 ± 1.9	103 ± 9
HB2	120	18	800	Fine	24.4	706 ± 36	33.3 ± 0.2	61.4 ± 2.3	25 ± 8
HB3	120	22	400	Fine	24.4	435 ± 6	13.1 ± 0.5	24.1 ± 1.8	99 ± 6
HB4	120	22	800	Coarse	24.4	555 ± 6	27.5 ± 0.2	50.7 ± 2.1	86 ± 3
HB5	180	18	400	Fine	24.4	412 ± 7	24.2 ± 0.1	44.6 ± 1.6	91 ± 5
HB6	180	18	800	Coarse	24.4	567 ± 35	34.2 ± 0.2	63.1 ± 2.5	64 ± 2
HB7	180	22	400	Coarse	24.4	292 ± 5	23.7 ± 0.1	43.8 ± 1.6	110 ± 2
HB8	180	22	800	Fine	24.4	415 ± 7	25.1 ± 0.2	46.3 ± 1.9	132 ± 11

then left overnight at room temperature (22 °C ± 1 °C) with continuous stirring. The next morning, the samples were reheated in a boiling water bath for 15 min, cooled, centrifuged at 12,000 × g for 15 min and filtered on a 0.45 μm filter. The filtrate (200 μL) was injected and eluted through two HR 10/30 columns packed with Sephacryl S-1000 connected in series with degassed 0.01 M aqueous NaOH at a flow rate of 10 mL h^{-1}, using a precision pump Pharmacia P-500. Samples were collected and the carbohydrate content was measured using the phenol-sulfuric acid method (Dubois, Gilles, Hamilton, Rebers, & Smith, 1956). The void volume and total elution volume were obtained by injecting waxy wheat starch (Sigma, S9679) and glucose (Sigma, 49139), respectively.

The extruded sample with the highest bran concentration and extruded with the highest specific mechanical energy value was hydrolyzed to glucose using a mixture of thermostable α-amylase (Megazyme, E-BLAAM) and amyloglucosidase (Megazyme, E-AMGDF). The hydrolyzate was run through the permeation column to validate that no fibers were eluted within the total elution volume. Analyzes were duplicated and the results were normalized according to the eluted total starch content (d.m.).

2.4. Total, soluble and insoluble dietary fiber content

The amount of the total dietary fibers (TDF) was measured according to AOAC 985.29 with minor modifications. Starch was gelatinized and partially hydrolyzed in a MES-TRIS buffer (pH 8.2) with a thermo-stable α-amylase (E-BLAAM, Megazyme Int. Wicklow, Ireland) at 95 °C for 30 min. Proteins were partially hydrolyzed with a protease (E-BSPRT, Megazyme Int. Wicklow, Ireland) at 60 °C for 30 min. After adjustment of pH to 4.5, residual starch was further hydrolyzed to glucose at 60 °C for 30 min with an amyloglucosidase (E-AMGDF, Megazyme Int. Wicklow, Ireland). Total dietary fibers were precipitated by adding four volumes of 95% ethanol, filtered and washed, while insoluble fiber (IDF) content was obtained by filtration after hydrolysis of starch and proteins followed by washing. After drying, protein and ash content were determined. Soluble fiber content (SDF) was obtained by difference. Measurements were done in duplicate.

2.5. Matrices solid state diagram

2.5.1. Sorption isotherms

Extruded samples were ground (particle size below 250 μm) and equilibrated at water activities (a_w) of 0.113, 0.225, 0.328, 0.432, 0.529 and 0.639, using LiCl, CH_3COOK, $MgCl_2$, K_2CO_3, $Mg(NO_3)_2$ and NaNO3 saturated salt solutions at 25 °C, respectively. Water sorption isotherms were assessed by measuring the water content corresponding to each water activity and calculated from the initial sample water content, measured by thermogravimetry (TG-DTA, Q600, TA Instruments, Crawley, United Kingdom), and maximum sample water gain or loss after 60 days. Experimental data were fitted with the Guggenheim–Anderson–de Boer model using the Excel solver function (Weisser, 1986):

$$W(a_w) = \frac{W_m C K a_w}{(1 - K a_w)(-K a_w + C K a_w)} \quad (5)$$

where C and K are constants and W_m is the monolayer water content on a dry basis.

2.5.2. Glass and melting temperatures

DSC thermographs were performed using a computer- and temperature controlled dynamic differential scanning calorimeter (model DSC 823e, Mettler Toledo, Greifensee, Switzerland). For each sample, 40 mg (d.m.) of the samples equilibrated at different water activities (see Section 2.5.1) were placed in a sealed mid-pressure aluminum pan (Mettler Toledo, Greifensee, Switzerland). Determination of the transitions was performed with Star System® v.6.01 software (Mettler Toledo, Switzerland). The water content in the samples ranged from 5.5% (w.b.) to 13.7% (w.b.).

For the starch melting temperature, the DSC program comprised a heating ramp from 10 °C to 250 °C at 5 K min^{-1}. The peak temperatures of the endothermic transitions were evaluated. Experimental points obtained for the melting temperature were fitted with the Flory–Huggins equation (Donovan, 1979):

$$\frac{1}{T} - \frac{1}{T^0} = \left(\frac{R}{\Delta H_u}\frac{V_2}{V_1}\right)[\nu - \chi_{12}\nu_1^2] \quad (6)$$

where R is the gas constant, ΔH_u is the enthalpy of fusion of the polymer per repeating unit, V_1 and V_2 are the molar volumes of

water and polymer, respectively, ν_1 and ν_2 are the volume fraction of water and polymer, T^0 is the transition temperature of the fully dried crystallites and χ_{12} is the Flory–Huggins interaction polymer-diluant parameter.

For glass transition temperature measurement, a temperature program was designed comprising heating from 5 °C to 140 °C at 5 K min^{-1}, cooling to 5 °C at 10 K min^{-1} and reheating to 150 °C at 5 K min^{-1}. For glass transitions below 50 °C, start and end temperatures of the heating ramps were set to −50 °C and 50 °C, respectively. Glass transition temperature was assessed during the second heating ramp at the transition onset $T_{g,\,onset}$, in duplicate. Experimental points for the glass transition temperature, obtained for each water activity, were fitted with the Gordon–Taylor equation using the Excel solver function (Gordon & Taylor, 1993):

$$T_g(W) = \frac{(100 - W)T_{g,m} + kWT_{g,w}}{(100 - W) + kW} \quad (7)$$

where W is the water content, $T_{g,m}$ and $T_{g,w}$ are the glass transition of the fully dried material and of pure water ($T_{g,w}$ = −139 °C, as suggested by Orford, Parker, & Ring, 1990), respectively and k is the Gordon–Taylor fitting parameter.

The dependency of the glass transition and melting temperatures according to the water activity was obtained by plotting the glass transition and melting temperatures calculated from the models given by Eqs. (6) and (7), against the water activity obtained from Eq. (5).

2.6. Experimental approach and statistical analysis

Two experimental plans were designed to investigate the main parameters driving the changes of the product properties. They also enabled to generate a wide range of product properties in a systematic way. A full factorial experimental plan of 8 experiments (numbered hereafter from 1 to 8) was designed to measure the effect of feed water content (18% and 22%), barrel temperature (120 °C and 180 °C) and screw speed (400 rpm and 800 rpm) on the water solubility (WSI) and absorption indices (WAI) of the refined wheat flour (RF, Table 1). A second factorial fractional experimental plan of 16 experiments was designed to investigate, additionally to the barrel temperature, feed water content and screw speed, the effect of bran particle size (fine and coarse) and fiber concentration (12.6% and 24.4%) (LB and HB, Table 1). The designs were balanced so that the level of each factor was tested in combination with the levels of the other factors. This ensured an independent and reliable estimation of the effect of each variable (Giesbrecht & Gumpertz, 2004). An analysis of variance was performed to evaluate the effect of each factor. This was followed by a multiple comparison test (least significant difference – LSD) to assess whether each level of a parameter was significantly different from the other level (Armitage & Colton, 1998). The full experimental plan on the refined wheat flour recipe and the fractional one according to the wheat bran concentration and particle size were analyzed separately. As no significant effect of the bran particle size was measured on WSI and WAI ($p < 0.05$) the results are presented according to the bran concentration.

3. Results and discussion

3.1. Starch physicochemical transformation

3.1.1. Water solubility and absorption indices

Negative trends were shown between the water absorption (WAI) and solubility indices (WSI), irrespective of the bran concentration (Fig. 1a). The water solubility index values were also positively correlated to the specific mechanical energy for the extruded refined flour (RF, $r^2 = 0.79$) and low bran concentration recipe (LB, $r^2 = 0.77$). They were nevertheless weakly correlated for the recipe with the highest bran concentration (HB, $r^2 = 0.29$) (Table 1). Both results were in agreement to previous reports on extruded cereals low in fibers in the elevated specific mechanical energy range (Schuchmann and Danner, 2000; Robin, Engmann, Pineau, et al., 2010). The authors explained it by a depolymerization of starch macromolecules, mainly amylopectins. As shown in Fig. 2, the increase in feed water content significantly decreased the water solubility index (WSI) and increased the water absorption index (WAI) for all recipes. This would be mainly due to a decrease in shear viscosity in the extruder with water content (Della Valle, Colonna, & Patria, 1996), resulting in a decreased amylopectin depolymerization. The increase in barrel temperature also decreased the water solubility index values for the refined wheat (RF) and low bran (LB) concentration recipes (Fig. 2). This may correspond to the decrease in the melt viscosity with temperature (Della Valle et al., 1996). An opposite trend with temperature was found for the recipe with the high bran (HB) concentration (Fig. 2). This recipe appeared to be affected differently by the temperature compared to the two other recipes. The increase in screw speed increased the water solubility index for all recipes, indicating an increased amylopectin depolymerization (Fig. 2). Increasing the screw speed decreases the shear viscosity of the shear thinning melt in the extruder (Della Valle et al., 1996; Horvat et al., 2009). Nevertheless, it also increases the shear stress transmitted to the starch molecules, resulting in an increased starch transformation extent (e.g. Barrès, Vergnes, Tayeb, & Della Valle, 1990).

3.1.2. RVA pasting profiles

The RVA pasting profiles of the unprocessed materials showed a peak of viscosity corresponding to the maximum swelling of non disrupted starch granules. The peak of viscosity measured for the refined wheat flour recipe (RF, $\eta = 2100$ cP) and indicating starch gelatinization, was only slightly reduced when increasing the bran concentration at the low level (LB, $\eta = 2000$ cP). It was drastically decreased when further increasing the bran to the higher concentration (HB, $\eta = 860$ cP). This is likely due to the change in recipe composition, with mainly a decrease in starch content when increasing the bran concentration. It also shows a non linearity of the RVA response with the starch concentration.

After extrusion, a peak of viscosity in the RVA profile could still be observed for all recipes. However it occurred at a shorter duration time than for the unprocessed material. A negative trend between the RVA peak viscosity of the extruded samples and the specific mechanical energy (SME) could be observed (Table 1 and Fig. 1b). The slope was steeper for the refined flour recipe (RF) than for the bran-containing recipes (LB and HB). Swelling of starch granules is mainly attributed to amylopectin structure and crystallinity (Tester & Morrison, 1990). DSC data (not shown here) depicted a total loss of the peak of starch gelatinization after extrusion, irrespective of the bran concentration and process conditions. According to these results, some amorphous starch structures that could swell in hot water remained after extrusion. The presence of such structures after cooking extrusion was rarely reported in the literature. Hagenimana, Ding, and Fang (2006) mentioned extruded rice-based material still able to swell under heat and an excess of water. They reported no remaining gelatinization peak by DSC after extrusion, suggesting that crystallinity had disappeared.

3.1.3. Estimated starch solubility

Adding bran to the extruded refined wheat flour shifted the trendline between the water absorption (WAI) and solubility (WSI) indices towards lower values (Fig. 1). The decrease in starch content with the bran concentration may explain these differences. The higher water solubility index values of the unprocessed recipes

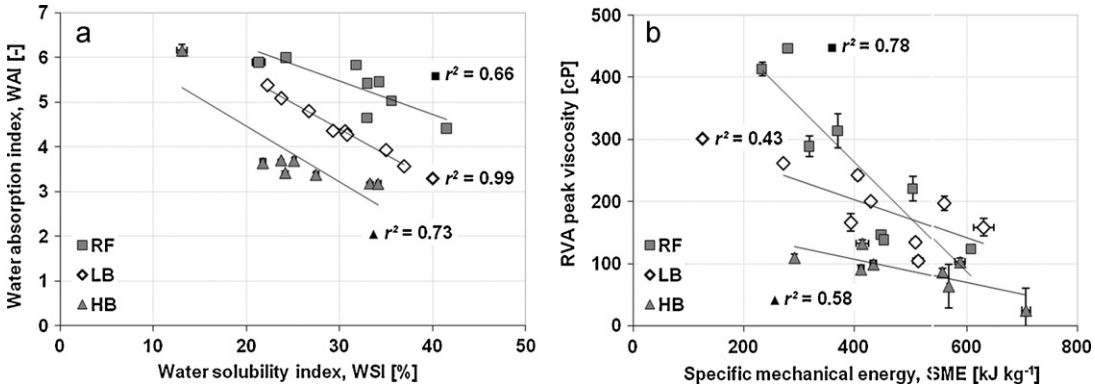

Fig. 1. (a) Water absorption index (WAI) vs. water solubility Index (WSI), b) RVA peak viscosity vs. specific mechanical energy (SME) (■ refined flour (RF); ◊ low bran concentration (LB); and ▲ high bran concentration (HB)).

when adding bran (7.1% ± 0.1%, 8.2% ± 0.2% and 9.7% ± 0.3% for RF, LB and HB, respectively) may also contribute to this difference. It also shows the higher solubility of the bran part compared to the wheat flour. The trendlines between the water absorption and solubility indices were nevertheless not perfectly fitting the experimental points. The differences between the water solubility index when increasing the bran level at same extrusion conditions were also not constant. Thus the decreased starch content and the higher solubility of the unprocessed products do not fully explain the differences in water solubility index between the extruded products at same process conditions. They may be attributed to an additional effect of the bran concentration on the solubilization extent of the recipe components (i.e. proteins, starch and fibers) during extrusion. This effect might be process conditions-dependant.

Increase in fiber and protein solubility during extrusion may depend on the recipe composition and process conditions. However, no significant change in soluble dietary fiber content (SDF) could be reported after extrusion, irrespective of the process conditions and recipes (Table 2). Additionally, protein solubility in water was shown to be low and reduced after extrusion (e.g. Falcone & Phillips, 1988; Yoshii, Furuta, Noma, & Noda, 1990; Lei & Lee, 1996). Considering that fiber and protein solubility were low, the water solubility index should be mainly determined by starch. Assuming that starch was mainly accounting for the water solubility index value, the percentage of starch water solubility according to the total starch content in the recipe could be estimated according to Eq. (4) (Table 1). The results showed that the starch water solubility values of the extruded samples without (RF) and with added bran at the intermediate concentration (LB) were close, except for conditions 6 and 8. The recipe with the highest bran concentration (HB) had higher starch water solubility values than the two other recipes (RF and LB), except for conditions 1 and 3. These differences in starch water solubility were process conditions-dependant. The highest differences between the two bran-containing recipes were obtained at the highest specific mechanical energy values (e.g. significant difference of 13% at 292 kJ kg^{-1} and 21% at 567 kJ kg^{-1}).

3.1.4. Starch molecular size distribution

Fig. 3a shows the gel permeation chromatography results of the unprocessed wheat flour and the extruded samples at two extreme conditions of specific mechanical energy (conditions 2: highest value and condition 7: lowest value). The unprocessed material showed two peaks of elution, a high molecular size peak, corresponding to amylopectin and one with a lower molecular size corresponding to amylose. The starch molecular size distribution was significantly modulated by the extrusion process (Fig. 3a). Irrespective of the composition, a unimodal distribution was observed after extrusion. This peak was shifted to lower molecular sizes with increasing SME value. At the lowest specific mechanical energy (condition 7), the distribution overlapped the amylopectin and amylose peaks (Fig. 3a). At the highest specific mechanical energy (condition 2) the amylopectin peak almost disappeared, resulting in a distribution closer to that of pure amylose (Fig. 3a). This supports the water absorption and solubility indices results (Section 3.1.1), tracing changes in extruded product behavior back to the depolymerisation of amylopectin branches, as also described by Davidson, Paton, Diosady, and Larocque (1984), Klingler, Meuser, & Niediek (1986), Politz, Timpa, White, and Wasserman (1994), Schuchmann and Danner (2000), Brümmer, Meuser, van Lengerich, and Niemann (2002). Some authors also reported an impact of

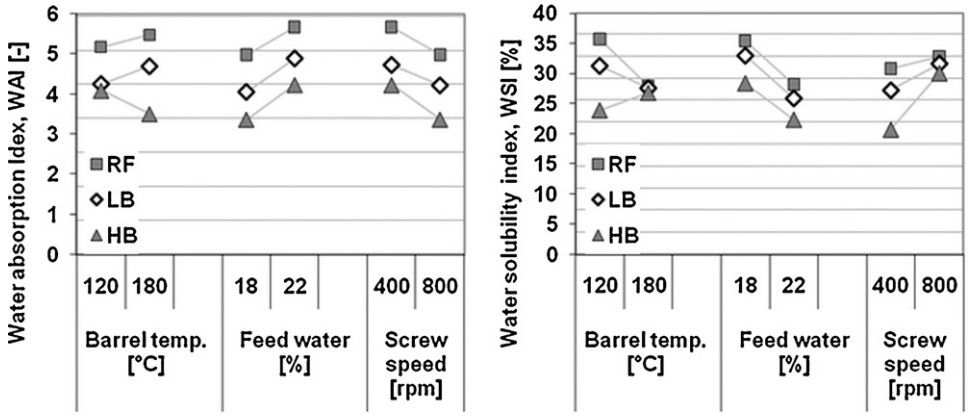

Fig. 2. Effect of process conditions on WAI and WSI (■ refined flour (RF); ◊ low bran concentration (LB); and ▲ high bran concentration (HB)) (the distance between two grid lines represents the least significant difference, LSD was 0.85 and 3.66% for WAI and WSI, respectively).

Table 2
Total (TDF), insoluble (IDF), soluble (SDF) dietary fibers content of raw and extruded samples at extremes of specific mechanical energy (SME).

	RF	RF7 233 kJ kg^{-1}	RF2 607 kJ kg^{-1}	LB	LB7 271 kJ kg^{-1}	LB2 630 kJ kg^{-1}	HB	HB7 292 kJ kg^{-1}	HB2 706 kJ kg^{-1}
TDF (% d.m.)	2.8 ± 0.2	2.8 ± 0.1	2.6 ± 0.5	12.6 ± 0.2	12.4 ± 0.9	13.9 ± 0.5	24.4 ± 0.2	23.5 ± 0.8	25.8 ± 1.7
SDF (% d.m.)	0.70 ± 0.04	0.9 ± 0.2	1.2 ± 0.5	1.9 ± 0.1	1.5 ± 0.3	2.2 ± 0.1	2.4 ± 0.5	2.1 ± 0.4	2.3 ± 0.5
IDF (% d.m.)	2.1 ± 0.1	1.88 ± 0.0	1.33 ± 0.4	10.8 ± 0.3	10.9 ± 1.2	11.7 ± 0.4	22.0 ± 0. 3	21.4 ± 1.2	22.9 ± 1.4

extrusion on both amylose and amylopectin (Colonna, Doublier, Melcion, de Monredon, & Mercier, 1984).

The molecular size distribution at different bran concentration but at same process conditions is compared in Fig. 3b and c. At the lowest specific mechanical energy (condition 7) and highest specific mechanical energy (condition 2), the elution profiles were very close, irrespective of the bran content. Nevertheless, at the highest specific mechanical energy (condition 2) a slight difference in molecular size distribution could be observed for the highest bran content (HB recipe) showing a shoulder peak close to the void volume (Fig. 3b). This could indicate remaining amylopectin chains (Fig. 3c). The close elution profile of the refined wheat flour and low bran recipes confirms that the starch transformation extent may be similar for these two recipes, as also indicated by close starch water solubility values.

The higher percentage of starch soluble starch (SWS) for the highest bran content compared to low or no bran containing recipes (LB and RF) at low SME (condition 7: SWS = 44% vs. 32% and 31%, respectively) and high SME (condition 2: SWS = 61% vs. 53% and 53%, respectively) (Table 1) might then be explained by the following hypothesis:

(i) The increased disruption of the previously mentioned amorphous structures which were shown to be able to hydrate and swell in hot water. This might lead to the release of some soluble starch molecules,

(ii) The generation of lower molecular weight carbohydrates in extrusion. On the gel permeation chromatographs of the extruded recipes (Fig. 3b and c), a peak close to the total elution volume could be observed. Its amplitude was increased with the bran concentration. This peak could be attributed to the bran fraction as shown on its gel permeation chromatograph (Fig. 3d). The generation of low molecular weight starch fractions during extrusion (likely resulting from amylopectin chains depolymerization) may overlap with this peak. It is however challenging to quantify them on the chromatographs.

3.2. Soluble and insoluble fibers content

Table 2 summarizes the total dietary fiber as well as the soluble and insoluble dietary fiber content of the unprocessed material and extruded samples at the two extreme conditions of specific mechanical energy (SME, condition 7: lowest SME and condition 2: highest SME). No significant change in total, soluble and insoluble dietary fibers could be observed after extrusion, irrespective of the bran concentration and process conditions (Table 2). Gualberto, Bergman, Kazemzadeh, and Weber (1997) observed no change in insoluble dietary fiber content, but an increase in soluble ones after extrusion of wheat bran. Also for wheat bran, Rallet, Thibault, and Della Valle (1990) reported a significant increase in soluble dietary fiber and a decrease in insoluble dietary fiber content. Considering the results reported for pure wheat bran in the literature and the

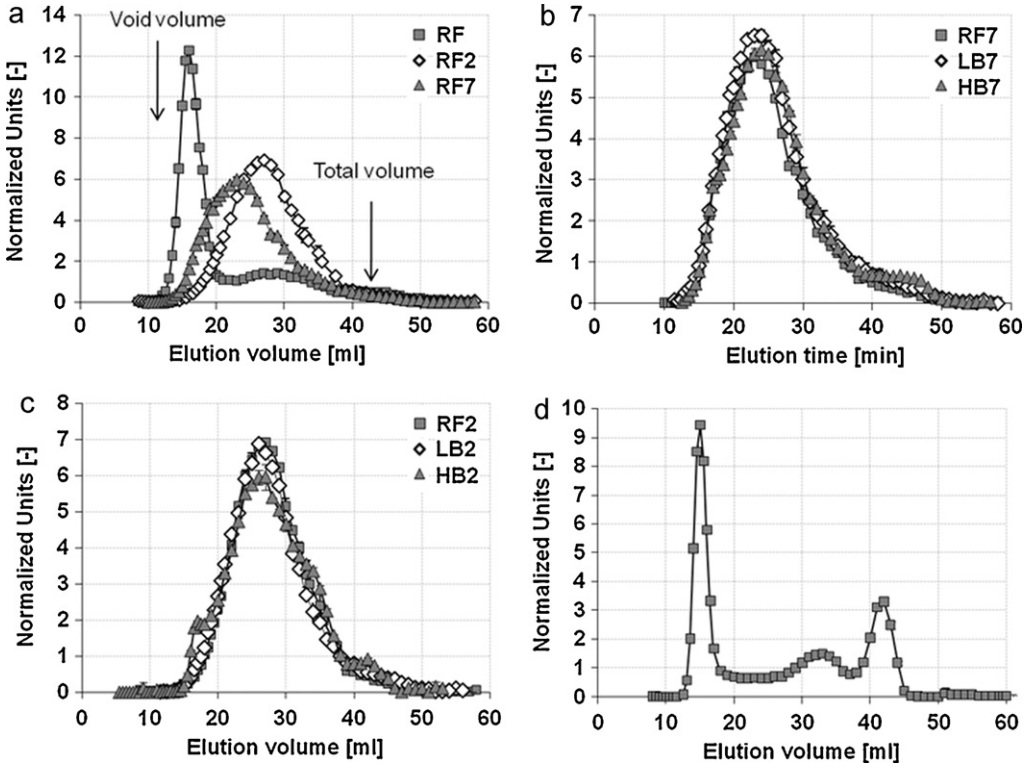

Fig. 3. Molecular size distribution of (a) Refined flour (■) unprocessed, (◊) extruded at condition 2, (▲) extruded at condition 7; (b) samples extruded at condition 2: (■) refined flour (RF), (◊) low bran concentration (LB), (▲) high bran concentration (HB); (c) samples extruded at condition 7: (■) refined flour (RF), (◊) low bran concentration (LB), (▲) high bran concentration (HB); and (d) unprocessed wheat bran.

ones found in this study, it appears that in the tested conditions starch had a protective effect on bran fibers. Nevertheless, Björck, Nyman, and Asp (1984) reported a significant increase in soluble dietary fiber and a decrease in insoluble dietary fiber content after extrusion of refined or whole wheat flours, which contains a smaller amount of wheat fibers. However, in all these studies the wheat source and analytical method differed.

3.3. Solid state diagrams

3.3.1. Melting temperature

The DSC thermographs for different water volume fractions (ν_1) are shown in Fig. 4 for different bran concentrations (a: RF, b: LB, c: HB) in comparison to pure wheat bran (d: WB). For the extruded refined flour recipe (RF), at $\nu_1 = 0.09$, a large multi-peak endothermic transition can be observed at a temperature of about 207 °C (Fig. 4a). The temperature at the peak shifts towards decreasing temperatures when increasing the water volume fraction. At the highest water volume fraction investigated ($\nu_1 = 0.20$), this endothermic peak is at about 161 °C. It becomes broader with water volume fraction, indicating more heterogeneous transitions. The temperature at the peak of the endothermic transition occurring at $\nu_1 = 0.20$ appears close the one reported by Jang and Pyun (1996) for wheat starch for a similar water volume fraction. The authors reported a peak at about 175 °C at 9.5% water content close to the value found in this study at 9.92% water content ($T_{pk} = 180$ °C). This peak was attributed to the combination of two peaks: one corresponding to the melting of starch crystallites (Burt & Russel, 1983) and a second one to the melting of the remaining crystallites or melting of amylopectin crystallites (Shogren, 1992). An additional shoulder can be detected at $\nu_1 = 0.12$ at about 205 °C, indicating the presence of different types of complexes (Fig. 4a). Two or more peaks with large enthalpies are found at the highest water volume fractions at about 200 °C. Endothermic peaks close or above 200 °C were also reported by Jang and Pyun (1996) for wheat starch in a similar range of water contents.

When adding bran at a low fiber concentration (LB), a similar trend to the one of the refined flour was observed (Fig. 4b). The temperature, at which the endothermic melting peak is found, is slightly decreased. It could hardly be detected at $\nu_1 = 0.18$ and 0.19. This may be due to the reduced starch content and/or overlap with other transitions associated with the starch or with the other flour components. For high bran content (HB) and pure wheat bran (WB), the endothermic peak with the largest enthalpy value decreases up to a water volume fraction ν_1 of 0.15 (Fig. 4c, d). It is not detectable any longer for higher water volume fractions (Fig. 4c, d). This endothermic transition may be attributed to the melting of starch crystallites. At same volume fraction of water, the peak temperature of this endothermic transition was lower for the high bran content and wheat bran material than for the refined flour or the low bran concentration recipe. This may indicate an effect of the bran fibers on the melting of starch crystallites. A similar effect of oat fibers on the melting of starch crystallites was reported by Núñez, Sandoval, Müller, Della Valle, and Lourdin (2009).

The temperature of the endothermic transition was determined for the different water contents at the peak (indicated by T_{pk} in Fig. 4) due to the difficulty of estimating the end of the transition (Fig. 5a). The standard deviations for T_{pk} and $T_{g,\,onset}$ did not exceed 4K. As expected from literature, T_{pk} decreases with water content. Although the Flory–Huggins Eq. (6) is better suited for water diluted starch systems, it was applied with fair agreements in several studies to more complex systems such as flours (e.g. Núñez et al., 2009; Champenois, Colonna, Buléon, Della Valle, & Renault, 1995). The experimental T_{pk} values of all recipes were plotted against the water volume fraction (Eq. (6)), even though only three points could be extracted from the DSC thermographs for the HB and wheat bran samples (Fig. 4). The relationship was very close to linearity and within the range of water volume fraction ($<\nu_1 = 0.7$) an approximation is accepted (Jang & Pyun, 1996). Therefore, the Flory-Huggins interaction polymer-diluent parameter (χ_{12}) was chosen to 0. The T_m^0 for this transition was extrapolated from the fit were close for refined flour (RF: 238 °C) or low bran concentration (LB: 236 °C) while they were lower for high bran content (HB: 198 °C) and wheat bran (WB: 186 °C).

3.3.2. Glass transition temperature

The glass transition temperature $T_{g,\,onset}$ related to the water content is reported in Fig. 5b. This transition can be mainly attributed to starch (Cuq, Abecassis, & Guilbert, 2003). As expected the $T_{g,\,onset}$ of the different recipes decreased with the increase in water content. The $T_{g,\,onset}$ values of the refined flour samples were lower than those reported by Kaletunç and Breslauer (1996) for wheat flour by Zeleznac and Hoseney (1987) for native wheat starch. Nevertheless in these studies the glass transition temperature was measured at the inflexion point of the transition. The experimental data were fitted with the Gordon–Taylor model (Eq. (7)) (Gordon & Taylor, 1993). From extrapolation the $T_{g,m}$ of the dry material was calculated. With increasing the bran concentration the $T_{g,m}$ values decreased from 194 °C to 105 °C. This was also true for increased water contents, where a linear relation between bran content and decrease in T_g was found. The $T_{g,m}$ for the refined flour extrapolated from the Gordon–Taylor model was lower than the value reported by Kaletunç and Breslauer (1996) and measured on a fully dried wheat flour (about 167 °C, measured at the inflexion point).

Although the hygrocapacity of refined flour (RF) and flour at low bran content (LB) are close, it is significantly reduced for high bran concentration (HB) and wheat bran (WB) (see sorption isotherms Fig. 5d). Increasing the bran concentration in the products mainly increases fibers and reduces starch concentration. The lower hygrocapacity of the bran-enriched recipes could therefore be attributed to the fibers which showed lower affinity with water compared to the other flour components. At the same water activity, the glass transition and melting temperatures were reduced when increasing the bran concentration (Fig. 5d). At same water content, the higher amount of the free water resulting from the increase in bran content led to both a reduction in glass transition and melting temperatures of starch (Fig. 5a, b). Effect of other cereal components, such as proteins (see Cuq et al., 2003) on the glass transition temperature may also interfere with the fibers effect.

3.3.3. Starch transformation

The extent of starch transformation according to the process conditions and bran content may be explained using the solid state diagrams (Fig. 5a, b). In cooking extrusion a combination of mechanical and thermal energy input transforms semi-crystalline starch into a plasticized, “molten” state, enabling the material to be formed, expanded and digested. Melting the material includes exceeding both the glass transition and melting temperature, with water acting mainly as “plasticizer”. The melting temperature at the peak and the glass transition temperature at 18% and 22% of water content in the feed were extrapolated from the Flory–Huggins (Eq. (6)) and Gordon and Taylor (Eq. (7)) models, respectively. At a barrel temperature of 180 °C, the melting temperature was exceeded for all samples (Fig. 5a and Table 3). At the lower barrel temperature of 120 °C, the melt temperature was in the same range as T_{pk} (Table 3). No crystallinity remained in all samples (see Section 3.1.2). This indicated a melt of the starch crystallites likely also induced by the shear in the extruder. Amorphous structures able to hydrate, swell and burst under shear in hot water were also found after extrusion (see Section 3.1.2). As the extrusion melt temperature was always well above $T_{g,\,onset}$ (Fig. 5b and Table 3), the molten starch matrix

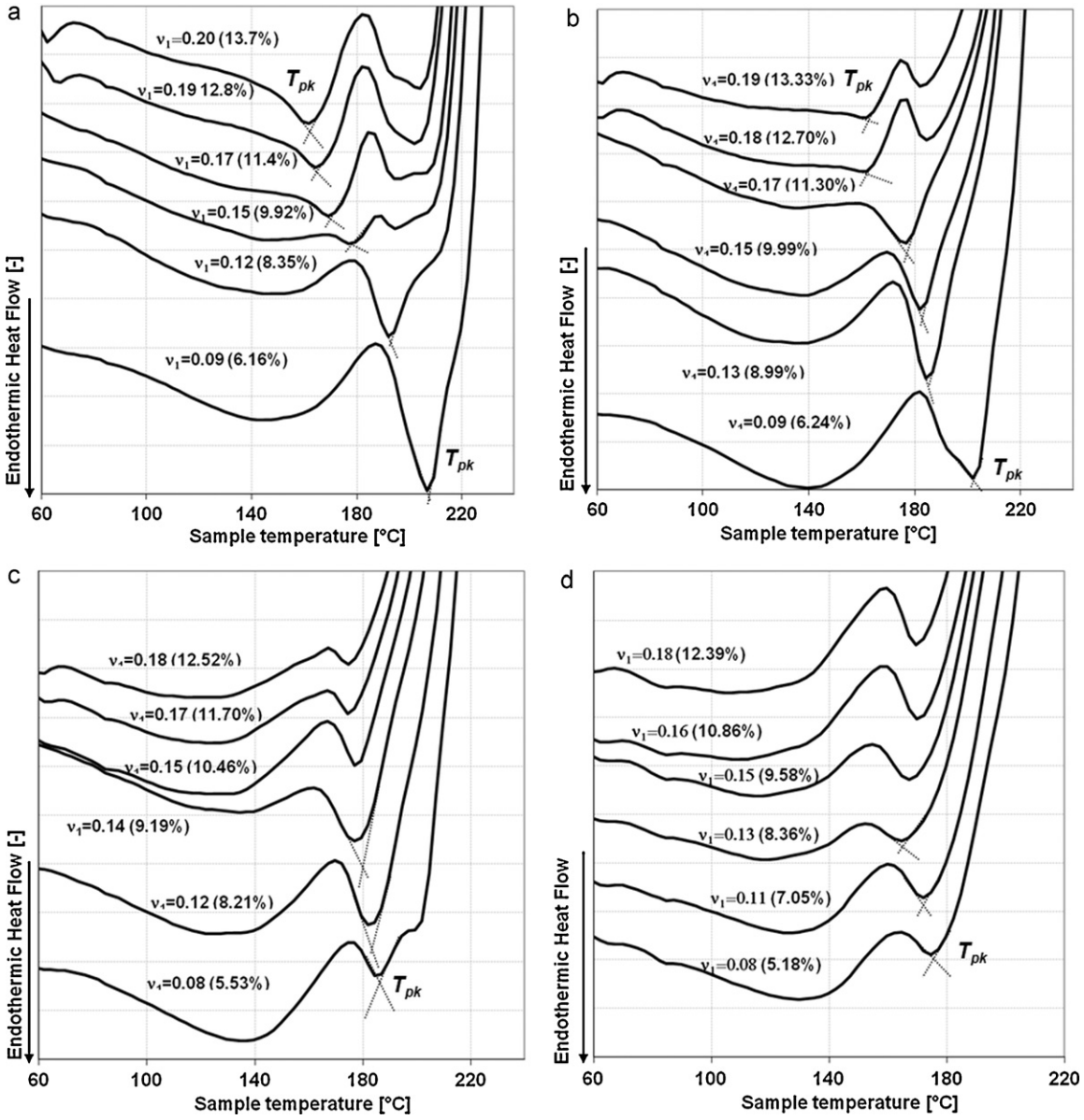

Fig. 4. DSC analysis: endothermic heat flow of unprocessed material according to the water volume fraction ν_1: (a) refined flour (RF); (b) low bran concentration (LB); (c) high bran concentration (HB); and (d) wheat bran (corresponding value of moisture content is given between parenthesis).

could move and deform freely in the extruder under shear. The presence of such structures may be attributed to the high pressure leading to compaction of the melt at the die exit and preventing their total disruption. The remaining swelling power of these structures might be linked to the amylopectin structure after extrusion that was showed to be mainly involved in the swelling capacity of native starch granules (Tester & Morrison, 1990).

Table 3
Product temperature measured at the die compared to the recipes melting (T_{pk}) and glass transition ($T_{g,onset}$) temperatures obtained from the modeling curves.

Recipe	Water content in the extruder (%)	Product temperature (T_d) (°C)	Estimated T_{pk} (°C)	Estimated $T_{g,\,onset}$ (°C)
RF	18	130–171	139	18
	22	118–171	121	−2
LB	18	131–180	139	8
	22	125–169	123	−12
HB	18	136–176	138	5
	22	127–171	128	−14

With increasing the bran concentration, the matrix glass transition temperature decreased but a difference in starch properties (see Section 3.1) was found only for the higher bran concentration. This might indicate a bran concentration threshold from which starch transformation starts to be modulated. This threshold may be attributed to several factors, being additive or counteracting each other:

(i) The reduction in glass transition temperature with bran content will result in a decreased starch viscosity at constant melt temperature (Williams, Landel, & Ferry, 1955). This might therefore reduce mechanical starch transformation in the extruder due to reduced mechanical stress.
(ii) The presence of insoluble bran particles may increase the matrix melt viscosity in the extruder as shown by Robin, Engmann, Tomasi, et al. (2010) at constant shear rate and indicated by the higher SME values obtained with this recipe (Table 1). This may lead to an increase in local mechanical stress with the starch molecules and to a higher starch transforma-

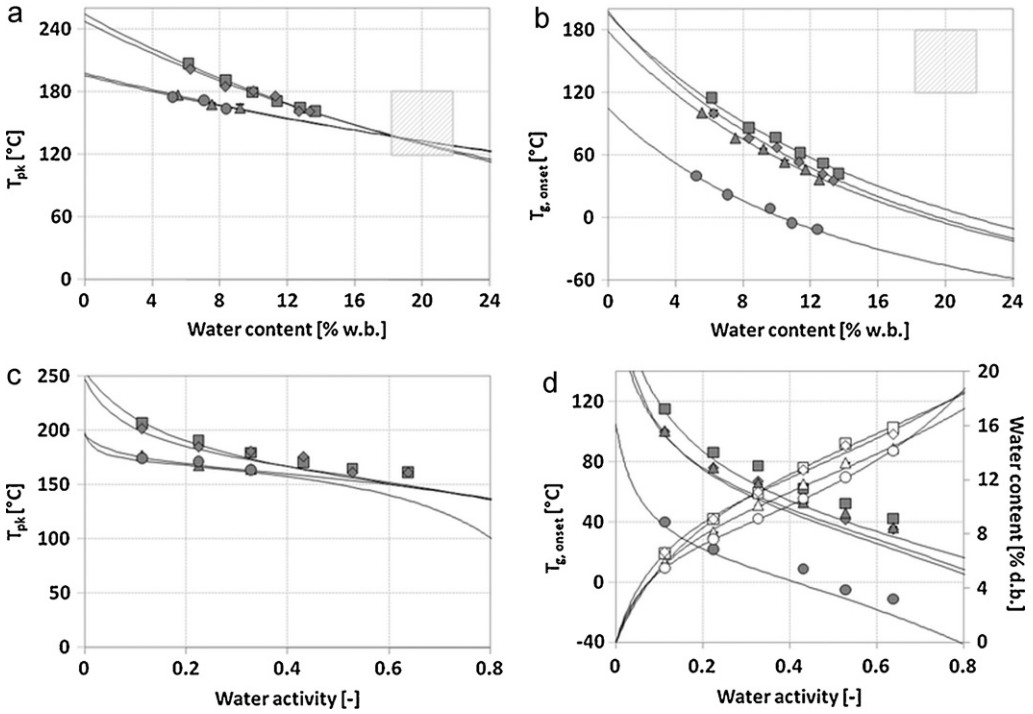

Fig. 5. Melting temperature T_{pk} and glass transition temperature $T_{g,\,onset}$ as a function of the water content (a and b), and as a function of water activity (c and d) of unprocessed recipes (■ refined flour (RF), ♦ low bran concentration (LB), ▲ high bran concentration (HB), ● wheat bran). Sorption isotherms are displayed figure d (□ refined flour (RF), ◊ low bran concentration (LB), △ high bran concentration (HB), ○ wheat bran) (The grey area represents the extrusion working domain).

tion. A decrease in bran particle size increases the surface of bran in contact with starch and may increase the extent of shear transmitted to the starch molecules. Nevertheless, no significant effect of the bran particle size on the water solubility and absorption indices was observed. This may be explained by the difference in average particle size of the fine and coarse bran. It may not be large enough to induce significant differences in starch transformation.

4. Summary and conclusions

Cooking extrusion of wheat flour enriched with wheat bran significantly modified the physicochemical properties of the starch. In the tested extrusion conditions, starch crystallites were fully dissociated. However, a remaining amorphous starch structure that could hydrate, swell and burst under shear in hot water was observed. Its extent decreased with the mechanical energy applied in the extruder. The estimated starch solubility was only increased at the highest bran concentration (HB). The bran content influenced the glass transition temperature, melting temperature and sorption isotherm of the unprocessed wheat flour. It showed that higher bran levels led to a higher amount of free water and a decrease in starch glass and melt temperatures. The differences in starch transformation, induced by the concentration of bran, might contribute to the modulation of the expansion properties of extruded starchy matrices containing wheat-bran. This will be the focus of future work.

Acknowledgments

The authors would like to thank Nestec S.A. for enabling and financing the work. Nicolas Bovet is acknowledged for the pilot plant experiments. The comments and review by Robert J. Redgwell and Sathaporn Srichuwong were highly appreciated.

References

Alvarez-Martinez, L., Kondury, K. P., & Harper, J. M. (1988). A general model for expansion of extruded products. *Journal of Food Science*, *53*(2), 609–615.
Anderson, R. A., Conway, H. F., Pfeifer, V. F., & Griffin, E. L. (1969). Gelatinization of corngrits by roll- and extrusion-cooking. *Cereal Science Today*, *14*(1), 4–11.
Armitage, P., & Colton, T. (1998). *Encyclopedia of biostatistics* UK: Wiley Editions., p. 1431.
Barrès, C., Vergnes, B., Tayeb, J., & Della Valle, G. (1990). Transformation of wheat flour by extrusion-cooking: influence of screw configuration and operating conditions. *Cereal Chemistry*, *67*, 427–433.
Björck, I., Nyman, M., & Asp, N.-G. (1984). Extrusion cooking and dietary fiber: Effects on dietary fiber content and degradation in the rat intestinal tract. *Cereal Chemistry*, *61*(2), 174–179.
Brennan, M., Monro, J. A., & Brennan, C. S. (2008). Effect of inclusion of soluble and insoluble fibres into extruded breakfast cereal products made with reverse screw configuration. *International Journal of Food Science and Technology*, *43*, 2278–2288.
Brümmer, T., Meuser, F., van Lengerich, B., & Niemann, C. (2002). Effect of extrusion cooking on molecular parameters of corn starch. *Starch/Stärke*, *54*(1), 9–15.
Burt, D. J., & Russel, P. L. (1983). Gelatinization of low water content wheat starch–water mixtures. *Starch/Stärke*, *35*, 354–360.
Champenois, Y., Colonna, P., Buléon, A., Della Valle, G., & Renault, A. (1995). Gélatinisation et rétrogradation de l'amidon dans le pain de mie. *Science des Aliments*, *15*, 593–614.
Colonna, P., Doublier, J. L., Melcion, J. P., de Monredon, F., & Mercier, C. (1984). Extrusion cooking and drum drying of wheat starch I. Physical and macromolecular modifications. *Cereal Chemistry*, *61*(3), 538–543.
Cuq, B., Abecassis, J., & Guilbert, S. (2003). State diagram to help describe wheat bread processing. *International Journal of Food Science and Technology*, *38*, 759–766.
Davidson, V. J., Paton, D., Diosady, L. L., & Larocque, G. (1984). Degradation of wheat starch in a single screw extruder: Characteristics of extruded starch polymers. *Journal of Food Science*, *49*, 453–458.
Della Valle, G., Colonna, P., & Patria. (1996). Influence of amylose content on the viscous behaviour of low hydrated molten starches. *Journal of Rheology*, *40*(3), 347–362.
Donovan, J. W. (1979). Phase transitions of the starch–water systems. *Biopolymers*, *18*, 263–275.
Dubois, M., Gilles, K. A., Hamilton, J. K., Rebers, P. A., & Smith, F. (1956). Colorimetric method for determination of sugars and related substances. *Analytical Chemistry*, *28*, 350.
Falcone, R. G., & Phillips, R. D. (1988). Effects of feed composition, feed moisture, and barrel temperature on the physical and rheological properties of snack-like products prepared from cowpea and sorghum. *Journal of Food Science*, *53*, 1464–1471.

Giesbrecht, F. G., & Gumpertz, M. L. (2004). *Planning, construction and statistical: Analysis of comparative experiments*. Hoboken, USA: Wiley Editions.

Gordon, M., & Taylor, J. (1993). Ideal copolymers and the second order transitions of synthetic rubbers: 1 Non crystalline copolymers. *Journal of Applied Chemistry*, *2*, 493–500.

Gualberto, D. G, Bergman, C. J., Kazemzadeh, M., & Weber, C. W. (1997). Effect of extrusion processing on the soluble and insoluble fiber, and phytic acid contents of cereal brans. *Plant Foods for Human Nutrition*, *51*, 187–198.

Hagenimana, A., Ding, X., & Fang, T. (2006). Evaluation of rice flour modified by extrusion cooking. *Journal of Cereal Science*, *43*, 38–46.

Horvat, M., Hirth, M., Emin, A., Schuchmann, H. P., Hochstein, B., & Willenbacher, N. (2009). Online-Rheologie zur Produktentwicklung extrudierter, funktioneller Zerealien. *Chemie Ingenieur Technik*, *81*(8), 1173–1180.

Jang, J. K., & Pyun, Y. R. (1996). Effect of moisture content on the melting of wheat starch. *Starch/Stärke*, *48*(2), S48–51.

Kaletunç, G., & Breslauer, K. J. (1996). Construction of a wheat-flour state diagram: application to extrusion processing. *Journal of Thermal Analysis*, *47*, 1267–1288.

Klingler, R. W., Meuser, F., & Niediek, E. A. (1986). Effect of the form of energy transfer on the structural charcateristics of starch. *Starch/Stärke*, *38*, 40–44.

Lei, M., & Lee, T.-C. (1996). Effect of extrusion temperature on solubility and molecular weight disruption of wheat flour proteins. *Journal of Agriculture Food Chemistry*, *44*, 763–768.

Marlett, M., McBurney, M. I., & Slavin, J. L. (2002). Position of the American Dietetic Association: Health implications of dietary fiber. *Journal of the American Dietetic Association*, *102*(7), 993–1000.

Núñez, M., Sandoval, A. J., Müller, A. J., Della Valle, G., & Lourdin, D. (2009). Thermal characterization and phase behavior of a ready-to-eat breakfast formulation and its starchy components. *Food Biophysics*, *4*, 291–303.

Orford, P. D., Parker, R., & Ring, S. G. (1990). Aspects of the glass transition behavior of mixtures of carbohydrates of low molecular weight. *Carbohydrate Research*, *196*, 11–18.

Politz, M. L., Timpa, J. D., White, A. R., & Wasserman, B. P. (1994). Non-aqueous gel permeation chromatography of wheat starch in deimethylacetamide (DMAC) and LiCl: Extrusion-induced fragmentation. *Carbohydrate Polymers*, *24*, 91–99.

Rallet, M.-C., Thibault, J.-F., & Della Valle, G. (1990). Influence of extrusion-cooking on the physico-chemical properties of wheat bran. *Journal of Cereal Science*, *11*, 249–259.

Robin, F., Engmann, J., Pineau, N., Chanvrier, H., Bovet, N., & Della Valle, G. (2010). Extrusion, structure and mechanical properties of complex starchy foams. *Journal of Food Engineering*, *98*, 19–27.

Robin, F., Engmann, J., Tomasi, D., Breton, O., Parker, R., Schuchmann, H. P., et al. (2010). Adjustable twin-slit rheometer for shear viscosity measurement of extruded complex starchy melts. *Chemical Engineering & Technology*, *33*(10), 1672–1678.

Schuchmann, H. P., & Danner, T. (2000). Product engineering using the example of extruded instant powders. *Chemical Engineering and Technology*, *23*(4), 303–308.

Shogren, R. L. (1992). Effect of moisture content on the melting and subsequent physical aging of corn starch. *Carbohydrate Polymers*, *19*, 83–90.

Tester, R. F., & Morrison, W. R. (1990). Swelling and gelatinization of cereal starches I. Effects of amylopectin, amylose, and lipids. *Cereal Chemistry*, *67*(6), 551–557.

Weisser, H. (1986). Influence of temperature on sorption isotherms. In M. Maguer, & P. Jelen (Eds.), *Transport phenomena*. London/New York, USA: Elsevier Science, Ltd.

Williams, M., Landel, R., & Ferry, J. (1955). The temperature dependence of relaxation mechanisms in amorphous polymers and other glass-forming liquids. *Journal of the American Chemical Society*, *77*, 3701–3707.

Yanniotis, S., Petraki, A., & Soumpasi, E. (2007). Effect of pectin and wheat fibers on quality attributes of extruded cornstarch. *Journal of Food Engineering*, *80*, 594–599.

Yoshii, H., Furuta, T., Noma, S., & Noda, T. (1990). Kinetic of Soy-protein denaturation by a temperature-programmed heat-denaturation technique. *Agricultural Biological Chemistry*, *54*, 863–869.

Zeleznac, K. J., & Hoseney, R. C. (1987). The glass transition of starch. *Cereal Chemistry*, *64*(2), 121–124.